Proceedings of the EuroGNC 2013, 2nd CEAS Specialist Conference
on Guidance, Navigation & Control, Delft University of Technology,
Delft, The Netherlands, April 10-12, 2013

Linear Quadratic Integrated vs. Separated Autopilot-Guidance Design*

Maital Levy, Tal Shima, and Shaul Gutman

Abstract Three types of guidance systems are studied. The first type is a separated two-loop autopilot guidance law that assumes spectral separation between the guidance and the flight control. However, separation may not hold close to interception, requiring possibly an integrated design of guidance and control. Using the integrated approach, two different guidance law types can be used to improve the end-game performance. The first one is the integrated single-loop guidance law, where the coupling between flight control and guidance loops is taken into account in the derivation process. The second type is the integrated two-loop autopilot guidance law. In this case, the autopilot loop is designed separately from the guidance one, but all the states are fed-back into the guidance loop. The performance of the three guidance laws is evaluated and compared via a single-input single-output test case. It is shown that the integrated two-loop autopilot-guidance law can manipulate the inner autopilot dynamics, resulting in the same performance as the integrated single-loop guidance law. In addition, it is shown that the performance of the separated guidance law is inferior to that of the integrated laws.

Maital Levy
Technion - Israel Institute of Technology, 32000 Haifa Israel, e-mail: maital@tx.technion.ac.il

Tal Shima
Technion - Israel Institute of Technology, 32000 Haifa Israel, e-mail: tal.shima@technion.ac.il

Shaul Gutman
Technion - Israel Institute of Technology, 32000 Haifa Israel, e-mail: mergutm@technion.ac.il

* This research was partially supported by the Technion Center for Security Science and Technology.

1 INTRODUCTION

The traditional approach to designing the guidance and flight control (G&C) system of interceptor missiles is using a decoupled architecture by assuming that spectral separation holds [1] . In this manner, the inner autopilot loop is stated as a solution of the infinite horizon tracking problem, where the reference signal is usually taken as an acceleration step command. And the outer guidance loop is designed based on a simplified low-order model of the autopilot dynamics. However, separation does not hold close to interception due to the rapid changes in the endgame geometry. This may cause instability and result in a miss distance increase. Integrated design of the G&C loops instead of separated design can improve the missile's performance due to the optimal integration of the G&C subsystems.

One of the most frequently used guidance laws, designed using a separated G&C approach, is proportional navigation (PN). This guidance law was proven to be the optimal guidance law in the case of an ideal dynamics missile and a nonmaneuvering target [2]. When the target is assumed to be performing a constant maneuver, the augmented proportional navigation (APN) is usually used instead. The APN guidance law is proportional navigation with an extra term accounting for the maneuvering target. When the ideal missile dynamics assumption is replaced by a first-order dynamics, the optimal guidance law (OGL)[3] is derived. This guidance law has a time-varying gain that requires a time-to-go estimator outside the guidance block.

A two-loop G&C system that is designed in one state space including both the missile dynamics and the engagement kinematics is denoted as an integrated two-loop autopilot-guidance law. In [4] a two-loop integrated G&C was designed using high order sliding mode control (SMC) and backstepping techniques. In the outer loop, the missile's pitch rate was used as the virtual control to keep the sliding quantity of the manifold close to zero. The inner loop was designed to enforce tracking of the pitch rate command in the presence of uncertainties.

A guidance loop that has to ensure the inner stability of the airframe as well as the target's interception is denoted as an integrated single-loop guidance law. An integrated single-loop G&C (IGC) problem was formulated in [5] as a finite-horizon dynamic game using partial-state information. The design objective was to obtain the controller that minimizes a given performance index under the worst-case target maneuvers and measurements disturbances. In [6] a class of PN guidance laws has been obtained in closed form by decoupling of the radial and tangential coordinates. Then, a typical transverse acceleration component of the PN guidance laws family was combined with the airframe dynamics to derive an autopilot control law. A time-delay control (TDC) method was used to design a single-loop IGC system in [7]. Using the TDC technique, the performance of the guidance law is dependent upon the controller's sampling time.

The following two integrated single-loop guidance laws have used the SMC technique for derivation. In [1] the SMC technique was applied to derive a controller for a canard controlled missile. The sliding surface was defined by a zero effort miss (ZEM) term obtained from the differential game formulation of the interception problem. The same methodology was used in [8] to obtain a controller for a dual

controlled missile. Motivated by the additional degree of freedom, offered by the two controllers, two sliding surfaces were defined to ensure good homing performance as well as a damped airframe response.

The feedback linearization technique was used in [9] for designing a single-loop integrated guidance and autopilot system. This technique is used for designing a nonlinear control system by transforming it into a linear, time invariant system with respect to its pseudo controller. Hence, the pseudo controller can be obtained by any linear design method. In this case, the infinite time horizon linear quadratic regulator (LQR) technique was combined with the feedback linearization method. A similar approach was employed in [10], only this time the transformed system was stated as a finite-interval problem. The latter was formulated in two ways. In the first approach, the problem was formulated as a finite-time problem. In the second one, the range was taken as the independent variable.

In this paper, three types of guidance laws are analyzed and compared: a separated two-loop autopilot guidance law, an integrated single-loop guidance law, and an integrated two-loop autopilot-guidance law. The guidance laws performance is studied using a thrust vector control (TVC) missile (taken from [11]) while imposing only zero miss distance. This is a single-input single-output (SISO) test case, where the scalar input is the missile's acceleration command and a single terminal cost is miss distance.

The remainder of this paper is organized as follows: In the next section, the problem formulation is presented. Then, in sections 3-4 the different guidance laws schemes and the test case description are presented. The simulations results are presented in Sec.5 followed by concluding remarks. In the Appendix, the solution of the finite-time regulator problem and the order reduction method are provided.

2 PROBLEM FORMULATION

The design assumptions will be next presented, followed by the set of linear equations of motion, and the interception scenario description.

2.1 Design Assumptions

The derivation of the guidance laws will be performed based on the following assumptions:

1. A skid-to-turn roll-stabilized missile is considered. The motion of such a missile can be separated into two perpendicular channels, thus allowing to treat only a planar motion.
2. Linear dynamics for both the evading target and the pursuing missile.

3. The missile's and target's deviations from the collision triangle are small during the end-game. In this manner, the relative end-game trajectory can be linearized about the nominal line of sight (LOS).
4. Constant speeds for both the missile and target.

2.2 Linear Equations of Motion

The general set of equations can be classified into three categories:

1. Kinematics (guidance) equations, $\mathbf{x_G} \in \mathscr{R}^{n_G \times 1}$
2. Dynamics equations, $\mathbf{x_D} \in \mathscr{R}^{n_D \times 1}$
3. Servo model equations [2] , $\mathbf{x_S} \in \mathscr{R}^{n_S \times 1}$

The dynamics equations are coupled to the servo equation but not vice versa

$$\begin{bmatrix} \dot{\mathbf{x}}_\mathbf{D} \\ \hline \dot{\mathbf{x}}_\mathbf{S} \end{bmatrix} = \left[\begin{array}{c|c} \mathbf{A_D} & \\ \hline [\mathbf{0}] & \mathbf{A_S} \end{array}\right] \begin{bmatrix} \mathbf{x_D} \\ \hline \mathbf{x_S} \end{bmatrix} + \begin{bmatrix} [\mathbf{0}] \\ \hline \mathbf{B_S} \end{bmatrix} \tilde{\mathbf{u}} \tag{1}$$

where $\tilde{\mathbf{u}} \in \mathscr{R}^{m \times 1}$ is the input to the servo and $[\mathbf{0}]$ is a matrix of zeroes with appropriate dimension. Note that $\mathbf{u} \in \mathscr{R}^{m_G \times 1}$ will denote the guidance controller. The matrix $\mathbf{A_D}$ may be rewritten as follows

$$\mathbf{A_D} = \left[\, \mathbf{A_{DD}} \middle| \mathbf{A_{DS}} \,\right] \tag{2}$$

where $\mathbf{A_{DD}} \in \mathscr{R}^{n_D \times n_D}$ and $\mathbf{A_{DS}} \in \mathscr{R}^{n_D \times n_S}$. The set of kinematic equations is given by

$$\dot{\mathbf{x}}_\mathbf{G} = \left[\, \mathbf{A_{GG}} \middle| \mathbf{A_{G,DS}} \,\right] \begin{bmatrix} \mathbf{x_G} \\ \hline \mathbf{x_D} \\ \mathbf{x_S} \end{bmatrix} \tag{3}$$

Finally, the general set of equations are given by

$$\dot{\mathbf{x}} = \mathbf{F}\mathbf{x} + \mathbf{G}\tilde{\mathbf{u}}, \quad \mathbf{x} = \left[\mathbf{x_G}\ \mathbf{x_D}\ \mathbf{x_S}\right]^T \tag{4}$$

where

$$\mathbf{F} = \left[\begin{array}{c|cc} \mathbf{A_{GG}} & \mathbf{A_{G,DS}} & \\ \hline [\mathbf{0}] & \mathbf{A_{DD}} & \mathbf{A_{DS}} \\ [\mathbf{0}] & [\mathbf{0}] & \mathbf{A_S} \end{array}\right], \quad \mathbf{G} = \begin{bmatrix} [\mathbf{0}] \\ \mathbf{B_S} \end{bmatrix} \tag{5}$$

[2] The equations of motion take into account the servo dynamics.

In its general form Eq. 4 is time varying. For simplicity of presentation the time dependency is not explicitly written.

2.3 End-Game Scenario Description

Figure 1 presents a schematic view of the planar endgame geometry where $X_{IF} - O_{IF} - Z_{IF}$ is a Cartesian inertial reference frame. X axis is aligned with the initial LOS, LOS_0, and Z axis is perpendicular to it. The subscripts P and E denote the pursuing missile and the evading target, respectively. V, a, and γ denote the speed, normal acceleration, and path angle. a_{PN}, and a_{EN} are respectively the pursuer and evader accelerations normal to LOS_0. r is the range between the adversaries and λ is the angle between the LOS and X_{IF} axis. y is the relative displacement between the target and the missile normal to X axis.

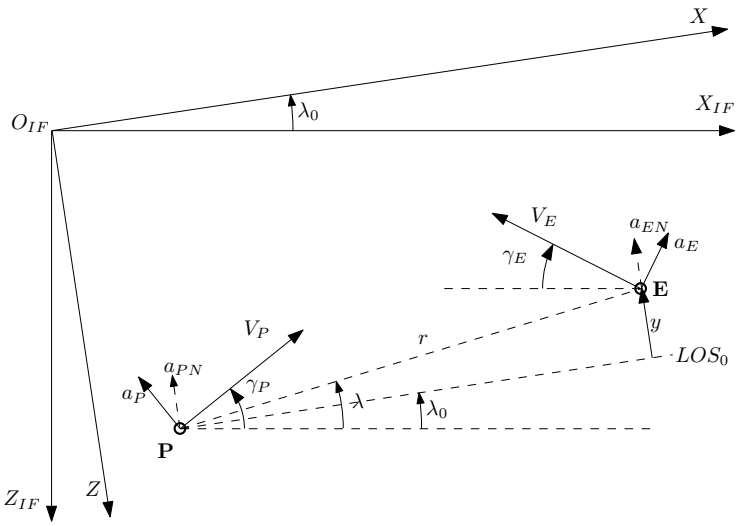

Fig. 1 Planar Engagement Geometry

The corresponding kinematic equation is

$$\ddot{y} = a_{EN} - a_{PN} \tag{6}$$

The pursuer's acceleration can be expressed as

$$a_{PN} = \mathbf{Cx} \tag{7}$$

3 AUTOPILOT-GUIDANCE DESIGN

3.1 Separated Two-Loop Autopilot-Guidance Law

Assuming spectral separation of the flight control and guidance loops allows to design them separately and use a decoupled G&C architecture as shown in figure 2. Thus, the outer guidance law loop can be treated as a solution of the finite horizon control problem and designed based on a simplified low-order model of the closed loop autopilot dynamics. The inner autopilot loop is stated as a solution to the infinite horizon control problem and is designed to follow the guidance acceleration commands.

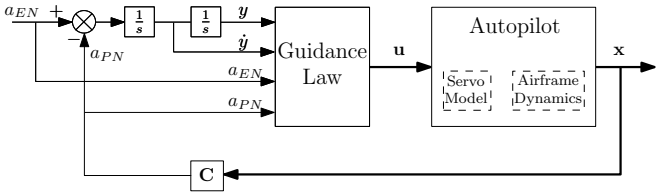

Fig. 2 Block Diagram of a Separated Two-Loop Autopilot-Guidance Law

Derivation of guidance laws based on a low-order approximation of the autopilot will be presented in sub-section 4.5.

3.2 Integrated Single-Loop Guidance Law

In the integrated design approach, the guidance law is being related directly to the dynamics of the airframe as presented in figure 3 [3]. In this way, the guidance law can use the information on the missile's internal states more effectively. Here, the solutions for the optimal controllers are the commands to the servo models, $\delta_{\mathbf{c}}$. The

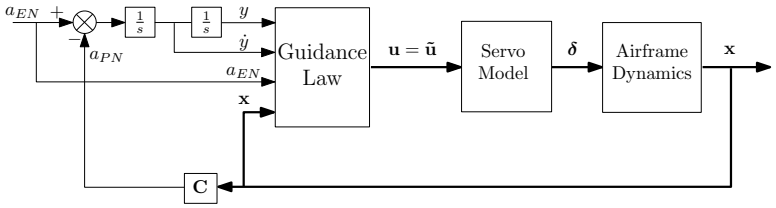

Fig. 3 Block Diagram of an Integrated Single-Loop Guidance Law

[3] It should be noted that the controller's deflection, δ, is part of the state vector, $\mathbf{x}$.

guidance law is stated as a solution to the finite time control problem. In an effort to meet the control requirements, different forms of cost functions can be chosen. In this case, a quadratic cost function is minimized

$$J = \mathbf{x}^T(t_f)\mathbf{Q_f}\mathbf{x}(t_f) + \int_{t_0}^{t_f} \mathbf{u}^T\mathbf{R}\mathbf{u}\, dt \tag{8}$$

The detailed solution to the finite time horizon problem is presented in the appendix. Substituting the optimal controller in the equations of motion (4) we obtain

$$\dot{\mathbf{x}} = \underbrace{\left[\mathbf{F} - \mathbf{G}\mathbf{R}^{-1}\mathbf{G}^{\mathbf{T}}\mathbf{P}\right]}_{\mathbf{F_I}}\mathbf{x}(\mathbf{t}) \tag{9}$$

where, $\mathbf{P}$ is the solution of the differential Riccati equation

$$-\dot{\mathbf{P}} = \mathbf{P}\mathbf{F} + \mathbf{F}^{\mathbf{T}}\mathbf{P} - \mathbf{P}\mathbf{G}\mathbf{R}^{-1}\mathbf{G}^{\mathbf{T}}\mathbf{P} \quad , \quad \mathbf{P}\left(t_f\right) = \mathbf{Q_f} \tag{10}$$

Remark 1. The presented approach of integrated single-loop guidance law is valid for linear systems. However, in practical missiles the controller deflection is bounded which requires treating a nonlinear system during saturation. In fact, during saturation the G&C loop is opened and if in addition the open loop transfer function is unstable or close to instability, the missile may be lost. In [12] this nonlinear effect was taken into account explicitely in designing a separated two-loop autopilot-guidance system. It was shown that in this case, the use of a decoupled diagram may achieve better performance than the integrated scheme.

3.3 Integrated Two-Loop Autopilot Guidance Law

The integrated two-loop autopilot guidance law has benefits of both the separated approach and the integrated approach. The inner autopilot is designed separately of the guidance law, but all the missile's states are fed back into the outer guidance loop as can be seen in figure 4.

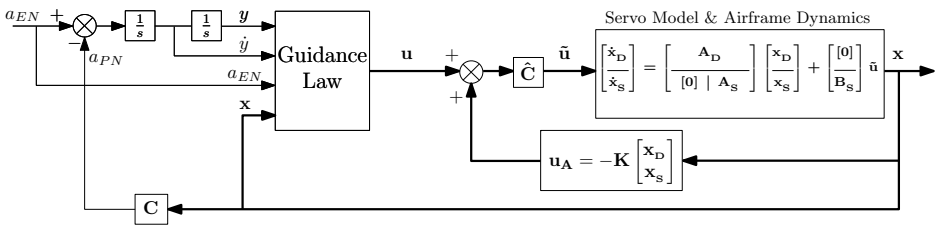

Fig. 4 Block Diagram of an Integrated Two-Loop Autopilot-Guidance Law

The autopilot's feedbacks can be equally described in controller terms

$$\mathbf{u_A} = -\mathbf{K}\begin{bmatrix}\mathbf{x_D}\\ \mathbf{x_S}\end{bmatrix}, \mathbf{K} = \begin{bmatrix}\mathbf{k_D} & \mathbf{k_S}\end{bmatrix} \tag{11}$$

where, $\mathbf{k_D} \in \mathscr{R}^{m_G \times n_D}$, $\mathbf{k_S} \in \mathscr{R}^{m_G \times n_S}$ and $\mathbf{u_A} \in \mathscr{R}^{m_G \times 1}$.
As can be seen in figure 4 the input to the missile's autopilot is not simply the guidance command, $\mathbf{u} \in \mathscr{R}^{m_G \times 1}$, but an equivalent controller that is given by

$$\tilde{\mathbf{u}} = \hat{\mathbf{C}}(\mathbf{u} + \mathbf{u_A}) = \hat{\mathbf{C}}\left(\mathbf{u} - \begin{bmatrix}\mathbf{k_D} & \mathbf{k_S}\end{bmatrix}\begin{bmatrix}\mathbf{x_D}\\ \mathbf{x_S}\end{bmatrix}\right) \tag{12}$$

where, $\hat{\mathbf{C}} \in \mathscr{R}^{m \times m_G}$ and $\tilde{\mathbf{u}} \in \mathscr{R}^{\mathbf{m}\times\mathbf{1}}$.
Thus, the running cost integral should be a function of $\tilde{\mathbf{u}}$

$$J = \mathbf{x}^{\mathbf{T}}(\mathbf{t_f})\mathbf{Q_f}\mathbf{x}(\mathbf{t_f}) + \int_t^{t_f} \tilde{\mathbf{u}}^{\mathbf{T}}(\tau)\tilde{\mathbf{R}}\tilde{\mathbf{u}}(\tau)\, d\tau \tag{13}$$

Substituting (12) in (4)-(5) the general set of differential equations is obtained

$$\dot{\mathbf{x}} = \mathbf{F_A}\mathbf{x} + \mathbf{G_A}\mathbf{u}, \quad \mathbf{x} = \begin{bmatrix}\mathbf{x_G} & \mathbf{x_D} & \mathbf{x_S}\end{bmatrix}^{\mathbf{T}} \tag{14}$$

where

$$\mathbf{F_A} = \left[\begin{array}{c|cc} \mathbf{A_{GG}} & \multicolumn{2}{c}{\mathbf{A_{G,DS}}} \\ \hline [\mathbf{0}] & \multicolumn{2}{c}{} \\ [\mathbf{0}] & \multicolumn{2}{c}{\begin{array}{cc}\mathbf{A_{DD}} & \mathbf{A_{DS}} \\ -\mathbf{B_S}\hat{\mathbf{C}}\mathbf{k_D} & \mathbf{A_S} - \mathbf{B_S}\hat{\mathbf{C}}\mathbf{k_S}\end{array}} \end{array}\right], \mathbf{G_A} = \begin{bmatrix}[\mathbf{0}]\\ \mathbf{B_S}\hat{\mathbf{C}}\end{bmatrix} \tag{15}$$

4 TEST CASE

The chosen test case is a TVC missile while minimizing a quadratic cost function with a terminal cost on the miss distance. First, the missile's model, the engagement kinematics, and the scenario parameters will be presented. Then, the corresponding autopilot design and guidance laws formulations will be presented.

4.1 Dynamics Model

The basic configuration of an Exo-atmospheric[4] TVC missile is given in figure 5. $X_{BF} - cg - Z_{BF}$ is a coordinate system parallel to the frame $X - O - Z$ (X axis is

[4] Outside the atmosphere, the atmospheric density is sufficiently low, therefore the aerodynamic forces and wind can be neglected.

aligned with the LOS_0 and Z axis is perpendicular to it), with its origin attached to the missile's center of gravity. $X_{BR} - cg - Z_{BR}$ is a rotating reference frame attached to the missile's center of gravity, where the X_{BR} axis is aligned with the missile's longitudinal axis. Let θ and δ_t denote the missile's body orientation and its thrust (tail controller) deflection, respectively. T is the thrust force and l_t is the distance from the center of mass to the nozzle.

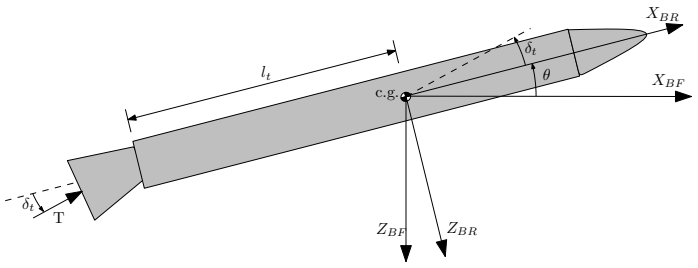

Fig. 5 Basic configuration of a TVC Missile

Projecting the thrust vector perpendicular to the missile's axis we get,

$$T_t = T \sin \delta_t$$

Using small angles approximation, i.e. $\sin \delta_t \cong \delta_t$ and $\cos \delta_t \cong 1$,

$$T_t \cong T \delta_t \tag{16}$$

The moment equation about the center of gravity is given by

$$I_{cg} \ddot{\theta} = -T_t l_t \tag{17}$$

where I_{cg} is the inertia moment about the center of gravity. Define

$$M_{\delta_t} = \frac{T l_t}{I_{cg}} \tag{18}$$

and using equation (16), one has

$$\ddot{\theta} = -M_{\delta_t} \delta_t \tag{19}$$

Taking only the thrust component perpendicular to the initial LOS

$$T \sin \phi = m a_{PN}, \quad \phi = \theta + \delta_t \tag{20}$$

And finally, by using small angle approximation, $\sin \phi \cong \phi$,

$$a_{PN} = \frac{T}{m} \phi \tag{21}$$

The state space formulation of the combined servo and dynamic model is given as follows

$$\begin{bmatrix} \dot{\mathbf{x}}_{\mathbf{D}} \\ \hline \dot{x}_S \end{bmatrix} = \left[\begin{array}{c|c} \mathbf{A}_{\mathbf{D}} & \\ \hline [\mathbf{0}] & A_S \end{array}\right] \begin{bmatrix} \mathbf{x}_{\mathbf{D}} \\ \hline x_S \end{bmatrix} + \begin{bmatrix} [\mathbf{0}] \\ \hline B_S \end{bmatrix} \tilde{u} \tag{22}$$

where the states are

$$\mathbf{x}_{\mathbf{D}} = \begin{bmatrix} \theta & \dot{\theta} \end{bmatrix}^T, \quad x_S = \delta_t, \quad \tilde{u} = \delta_t^c \tag{23}$$

and the model matrices are given by

$$\mathbf{A}_{\mathbf{D}} = \begin{bmatrix} 0 & 1 & 0 \\ 0 & 0 & -M_{\delta_t} \end{bmatrix}, \quad A_S = -\frac{1}{\tau_t}, \quad B_S = \frac{1}{\tau_t} \tag{24}$$

Remark 2. In a TVC missile, the velocity, mass and inertia are time varying. However, since the guidance law is designed for the end-game phase they can be assumed to be nearly constant.

4.2 Kinematics Equations

Assuming perfect information of the future target's maneuver strategy and that it is to perform a constant maneuver, we have

$$\dot{a}_E = 0 \tag{25}$$

Using (25) and (6), the kinematics state space formulation is given by

$$\begin{aligned} \mathbf{x}_{\mathbf{G}} &= \begin{bmatrix} y & \dot{y} & a_{EN} \end{bmatrix}^T \\ \mathbf{A}_{\mathbf{GG}} &= \begin{bmatrix} 0 & 1 & 0 \\ 0 & 0 & 1 \\ 0 & 0 & 0 \end{bmatrix}, \mathbf{A}_{\mathbf{G,DS}} = \begin{bmatrix} [\mathbf{0}] \\ -\mathbf{C} \\ [\mathbf{0}] \end{bmatrix} \end{aligned} \tag{26}$$

4.3 Scenario Parameters

Table 1 presents the scenario parameters.

Table 1 Scenario Parameters Values

Parameter	Value	Units
τ_t	0.1	sec
T/m	120	m/sec^2
a_{EN}	10	m/sec^2
y_0	10	m
M_{δ_t}	200	$1/sec^2$

4.4 Autopilot Design

Figure 6 presents the TVC missile autopilot scheme that ensures zero steady-state error to constant acceleration command inputs.

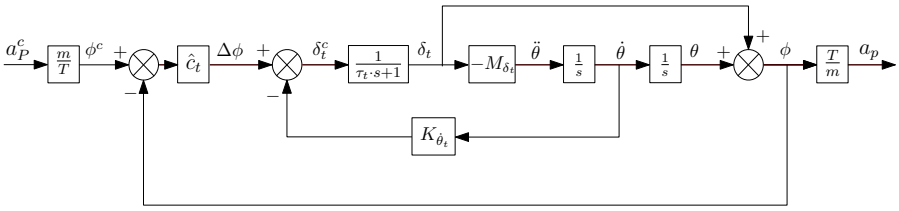

Fig. 6 TVC Missile - Autopilot Block Diagram

Table 2 provides the design gains of the tail controller. From now on, the phrase **autopilot version X** will relate to gain set number X.

Table 2 Tail Controller Design Gains

Gain Set	$K_{\dot{\theta}_t}$	$\hat{c}_t$
0.	-0.0413	-0.1644
1.	-0.0347	-0.1219
2.	-0.0347	-0.1026

4.5 Separated Two-Loop Autopilot Guidance Law Formulation

The design of a separated two-loop autopilot guidance law is based on a low-order approximation of the autopilot dynamics. Thus, the closed form solution of the guidance law will be obtained assuming ideal autopilot dynamics and a constant maneuvering target. The state-space form of the equation set is given in equation 26, where

$$\mathbf{F} = \mathbf{A_{GG}}, \quad \mathbf{G} = \begin{bmatrix} 0 \\ -1 \\ 0 \end{bmatrix}, \quad \mathbf{x} = \mathbf{x_G} \tag{27}$$

The chosen weight matrices are

$$R = 1, \quad \mathbf{Q_f} = \mathbf{Q_f} = \mathbf{M^T M} = \begin{bmatrix} a^2 & 0 & 0 \\ 0 & 0 & 0 \\ 0 & 0 & 0 \end{bmatrix} \Rightarrow \mathbf{M} = \begin{bmatrix} a & 0 & 0 \end{bmatrix} \tag{28}$$

The problem's order was reduced (see the appendix) in order to obtain the closed-form solution

$$\begin{aligned} &\mathscr{P} = \left(1 + a^2 \frac{t_{go}^3}{3}\right)^{-1} \\ &z(t_{go}) = C_z \cdot \mathscr{P}^{-1}, \quad C_z = \frac{z_0}{1 + a^2 \frac{t_f^3}{3}} \\ &a_P^c = C_z a t_{go} \end{aligned} \tag{29}$$

where z_0 is the initial zero effort miss given by

$$z_0 = a\left(x_1(0) + t_f x_2(0) + \frac{t_f^2}{2} x_3(0)\right)$$

4.6 Integrated Single-Loop Guidance Law Formulation

In sub-section 3.2, the integrated single-loop guidance law's optimization problem is formulated. This formulation will be applied to the TVC missile case. It should be noted that the integrated single-loop guidance law command is the thrust deflection.

Using the TVC model equations (22-24) and the kinematics equations (3,26), the state-space form of the equation set is given by

$$\mathbf{x} = \begin{bmatrix} y & \dot{y} & a_{EN} & \theta & \dot{\theta} & \delta_t \end{bmatrix}^T, \quad \tilde{u} = u = \delta_t^c \tag{30}$$

$$\begin{aligned} &\mathbf{F} = \begin{bmatrix} \mathbf{F_{11}} & \mathbf{F_{12}} \\ [\mathbf{0}] & \mathbf{F_{22}} \end{bmatrix}, \quad \mathbf{F_{11}} = \begin{bmatrix} 0 & 1 & 0 \\ 0 & 0 & 1 \\ 0 & 0 & 0 \end{bmatrix}, \quad \mathbf{F_{12}} = \begin{bmatrix} 0 & 0 & 0 \\ -\frac{T}{m} & 0 & -\frac{T}{m} \\ 0 & 0 & 0 \end{bmatrix} \\ &\mathbf{F_{22}} = \begin{bmatrix} 0 & 1 & 0 \\ 0 & 0 & -M_{\delta_t} \\ 0 & 0 & -\frac{1}{\tau_t} \end{bmatrix}, \quad \mathbf{G} = \left[[\mathbf{0}] \,\middle|\, \frac{1}{\tau_t} \right]^T \end{aligned} \tag{31}$$

The chosen weight matrices are

$$R = 1, \quad \mathbf{Q_f} = \begin{bmatrix} a^2 & [\mathbf{0}] \\ [\mathbf{0}] & [\mathbf{0}] \end{bmatrix} \tag{32}$$

4.7 Integrated Two-Loop Autopilot Guidance Law Formulation

In sub-section 3.3, the integrated two-loop autopilot guidance law's optimization problem was formulated. This formulation will be applied to the current test case. In this case, the input to the missile's autopilot is an equivalent controller that is given by

$$\tilde{\mathbf{u}} = \hat{\mathbf{C}}(\mathbf{u} + \mathbf{u_A}) = \hat{\mathbf{C}}\left(\mathbf{u} - \begin{bmatrix} \mathbf{k_D} & \mathbf{k_S} \end{bmatrix} \begin{bmatrix} \mathbf{x_D} \\ \mathbf{x_S} \end{bmatrix}\right) = \mathbf{C_{eq}x} + \mathbf{D_{eq}u}$$

The cost function is

$$J = \mathbf{x^T}(\mathbf{t_f})\mathbf{Q_f x}(\mathbf{t_f}) + \int_t^{t_f} \tilde{\mathbf{u}}^{\mathbf{T}}(\tau)\tilde{\mathbf{R}}\tilde{\mathbf{u}}(\tau)\, d\tau$$

where the running cost term can be equally expressed by

$$\tilde{\mathbf{u}}^{\mathbf{T}}\tilde{\mathbf{R}}\tilde{\mathbf{u}} = \mathbf{u^T R u} + \mathbf{2x^T S u} + \mathbf{x^T Q x}$$
$$\mathbf{x} = \begin{bmatrix} \mathbf{x_G} & \mathbf{x_D} & \mathbf{x_S} \end{bmatrix}^T$$

Hence, the appropriate running cost weight matrices are given by

$$\mathbf{Q} = \begin{bmatrix} [\mathbf{0}] & [\mathbf{0}] \\ [\mathbf{0}] & \mathbf{C_{eq}^T}\tilde{\mathbf{R}}\mathbf{C_{eq}} \end{bmatrix}, \quad \mathbf{S} = \begin{bmatrix} [\mathbf{0}] \\ \mathbf{C_{eq}^T}\tilde{\mathbf{R}}\mathbf{D_{eq}} \end{bmatrix}, \quad \mathbf{R} = \mathbf{D_{eq}^T}\tilde{\mathbf{R}}\mathbf{D_{eq}} \tag{33}$$

In this case, the guidance commands are the acceleration commands and not the controller deflection commands. Therefore, in order to get the appropriate deflection command, ϕ^c, the guidance command has to be multiplied by $\frac{m}{T}$ ($\phi^c = \frac{m}{T}a_P^c$).

The equivalent controller is obtained from the autopilot block diagram presented in figure 6

$$\tilde{u} = \hat{c}_t \frac{m}{T} u - \begin{bmatrix} \hat{c}_t & K_{\dot{\theta}_t} & \hat{c}_t \end{bmatrix} \begin{bmatrix} \theta \\ \dot{\theta} \\ \delta_t \end{bmatrix} \tag{34}$$

where u is the guidance acceleration command.
Using the TVC model equations (22-24) and the kinematics equations (3,26), the state-space form is

$$\mathbf{x} = \begin{bmatrix} y & \dot{y} & a_{EN} & \theta & \dot{\theta} & \delta_t \end{bmatrix}^T, \quad u = a_P^c \tag{35}$$

$$\mathbf{F_A} = \begin{bmatrix} \mathbf{F_{A11}} & \mathbf{F_{A12}} \\ [\mathbf{0}] & \mathbf{F_{A22}} \end{bmatrix}, \quad \mathbf{F_{A11}} = \begin{bmatrix} 0 & 1 & 0 \\ 0 & 0 & 1 \\ 0 & 0 & 0 \end{bmatrix}, \quad \mathbf{F_{A12}} = \begin{bmatrix} 0 & 0 & 0 \\ -\frac{T}{m} & 0 & -\frac{T}{m} \\ 0 & 0 & 0 \end{bmatrix}$$
$$\mathbf{F_{A22}} = \begin{bmatrix} 0 & 1 & 0 \\ 0 & 0 & -M_{\delta_t} \\ -\frac{\hat{c}_t}{\tau_t} & -\frac{K_{\dot{\theta}_t}}{\tau_t} & -\frac{(1+\hat{c}_t)}{\tau_t} \end{bmatrix}, \quad \mathbf{G_A} = \left[[\mathbf{0}] \ \frac{m}{T}\frac{\hat{c}_t}{\tau_t} \right]^T \tag{36}$$

The chosen weight matrices are

$$\tilde{R} = 1, \quad \mathbf{Q_f} = \begin{bmatrix} a^2 & [\mathbf{0}] \\ [\mathbf{0}] & [\mathbf{0}] \end{bmatrix} \tag{37}$$

5 SIMULATION RESULTS

In this section both the separated two-loop autopilot-guidance law and the integrated two-loop autopilot-guidance law will be compared to the integrated single-loop guidance law. The integrated single-loop guidance law uses a combined state space of the kinematics and airframe dynamics. In this way, the guidance law is able to take into account the missile's dynamics most efficiently. Thus, the integrated single-loop guidance law is expected to achieve the optimal performance subject to a given missile's model and may be used as a proper benchmark system to evaluate the other guidance laws' performance. The results of the two-loop type guidance laws will be computed for all three autopilot versions presented in table 2.

5.1 Separated Two-Loop Autopilot Guidance Law vs. Integrated Single-Loop Guidance Law

The simulations results will be summarized via a Pareto Front curve. Each point on the curve is a simulation result with a different miss distance weight in terms of the squared miss distance, $y^2(t_f)$, and the tail control effort, $\int \delta_t{}^c(t)^2 dt$. And so, when $a \to \infty$ the miss distance is decreased and the control effort is increased. The obtained curve presents the optimal performance that may be achieved subject to a given airframe model. Being below the Pareto Front is not possible, since the optimal results cannot be improved and being above it means the obtained results are not optimal.

Figure 7 presents the Pareto Front curves of both the integrated single-loop guidance law and of the separated two-loop autopilot-guidance law. As expected, the separated guidance law curves appear above the integrated guidance law curve. The integrated guidance law was designed based on the full missile's model, whereas the separated guidance law was derived assuming ideal missile's dynamics. Therefore, it was not able to predict accurately the airframe response and issue the appropriate

guidance command. Moreover, the separated guidance law uses only information on the kinematical states, whereas the integrated one uses all the states (kinematic and dynamics).

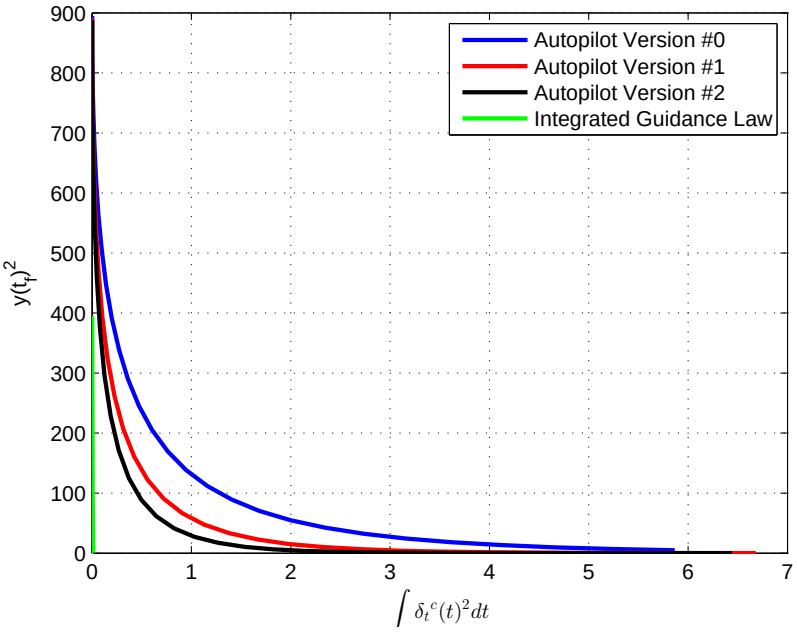

Fig. 7 Pareto Front - Separated Guidance Law & Integrated Single-Loop Guidance Law

5.2 Integrated Two-Loop Autopilot Guidance Law vs. Integrated Single-Loop Guidance Law

In this case the simulations results will be presented via Pareto Front and sample runs.

Pareto Front

Figure 8 presents a Pareto Front of an integrated single-loop guidance law and of an integrated two-loop autopilot guidance law. The results of the integrated single-loop guidance law and of the integrated two-loop guidance law coincide for all three autopilot versions. The integrated two-loop autopilot guidance law was able to take

into account the autopilot inner-dynamics due to the full-state feedback incorporated in the block diagram (figure 4).

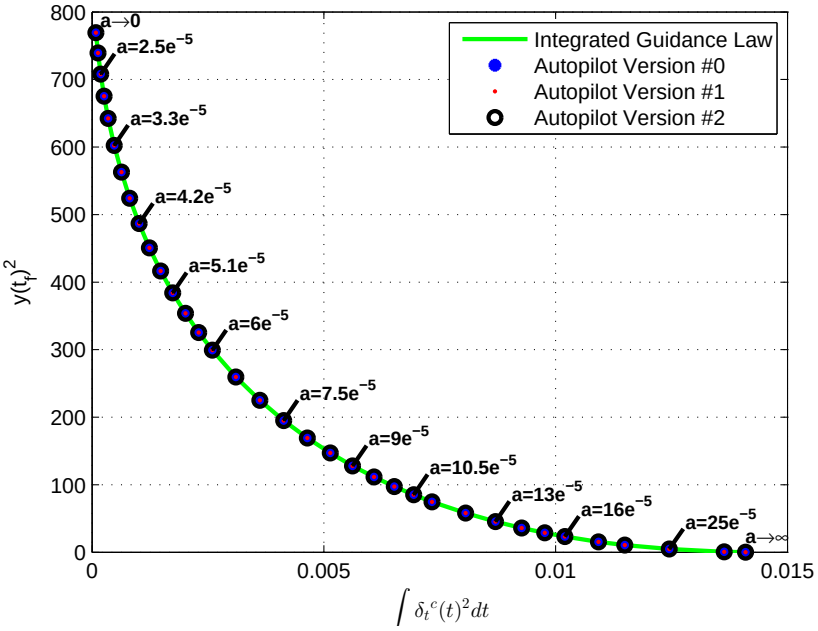

Fig. 8 Pareto Front - Integrated Guidance Laws

Sample Runs

Figure 9 presents the deflection commands of both guidance laws. In the integrated single-loop guidance law, the guidance command is directly the deflection command. Whereas in the integrated two-loop guidance law, the guidance command is an acceleration command that has to be followed by the autopilot. In this manner, only the equivalent controller (equation 12) is the input to the servo model. Therefore, to obtain the same cost, only the equivalent acceleration command of the integrated two-loop autopilot-guidance law must have the same values as the guidance deflection command of the integrated single-loop guidance law. Figure 10 presents the kinematic states. It can be seen that the miss distance is nulled at the end of the interception for the given weight, $a = 3 \cdot 10^{-4}$.

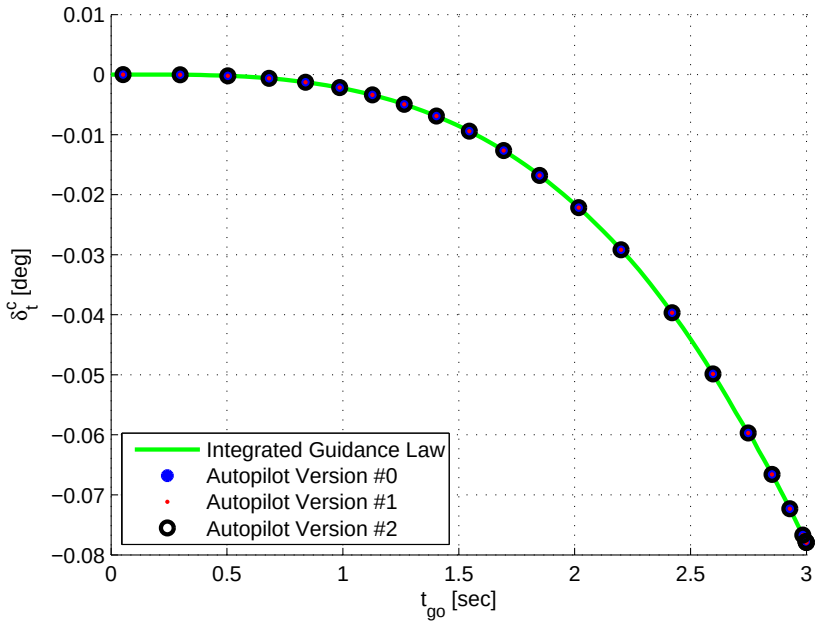

Fig. 9 Deflection Commands - Integrated Guidance Laws ($a = 3 \cdot 10^{-4}$)

6 CONCLUSIONS

In this paper, three types of guidance laws were studied: separated two-loop autopilot-guidance law, integrated two-loop autopilot-guidance law, and integrated single-loop guidance law. The integrated single-loop guidance law was used as a benchmark system to evaluate the other guidance laws performance, since it is expected to achieve the optimal performance subject to a given missile's model. The performance of the different guidance laws was analyzed through simulations by using the concept of Pareto Front and sample runs. The simulations were held for SISO test case that is a TVC missile model where only zero miss distance is imposed. It was shown that the performance of the integrated guidance law is superior to the separated one. In the separated approach, the guidance law is designed based on a low order missile's model and therefore cannot issue the appropriate guidance command. The integrated two-loop autopilot-guidance law was shown to achieve the same performance as the integrated single-loop guidance law. This may be explained by the full-state feedback to the integrated two-loop autopilot-guidance law that enables taking into account the autopilot inner-dynamics.

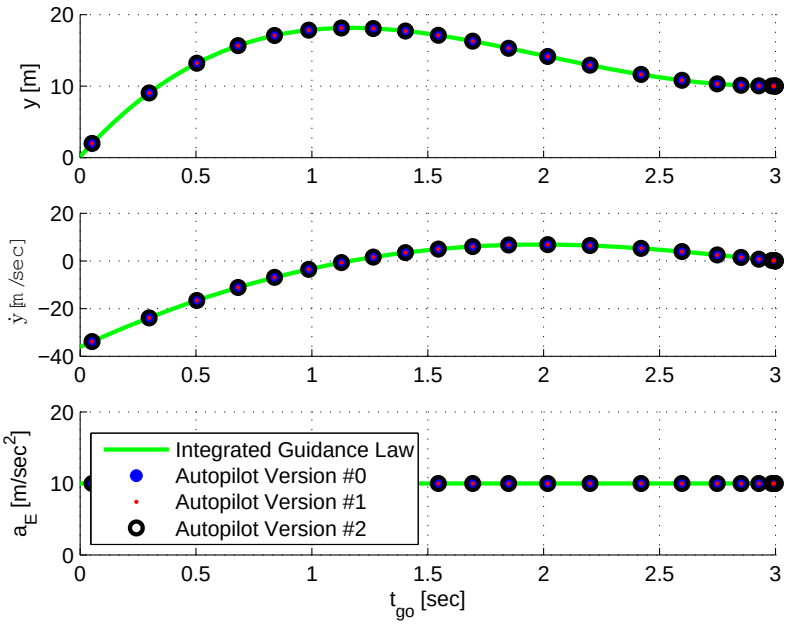

Fig. 10 Kinematic States - Integrated Guidance Laws ($a = 3 \cdot 10^{-4}$)

7 APPENDIX: SOLUTION of the FINITE-TIME REGULATOR PROBLEM[13]

Consider the linear time variant system

$$\dot{\mathbf{x}}(\mathbf{t}) = \mathbf{F}(\mathbf{t})\mathbf{x}(\mathbf{t}) + \mathbf{G}(\mathbf{t})\mathbf{u}(\mathbf{t}) \qquad \mathbf{x}(t_0) \text{ given} \tag{38}$$

where $\mathbf{x}(t) \in \mathscr{R}^n$ is the state vector, $\mathbf{u}(t) \in \mathscr{R}^m$ is the control vector, $\mathbf{F}(t) \in \mathscr{R}^{n\times n}$, $\mathbf{G}(t) \in \mathscr{R}^{n\times m}$ are weight matrices.

The minimization problem is the task of finding the optimal controller $\mathbf{u}^*(t), t \in [t_0, t_f]$, which minimizes

$$J = \mathbf{x}^{\mathbf{T}}(\mathbf{t_f})\mathbf{Q_f}\mathbf{x}(\mathbf{t_f}) + \int_{t_0}^{t_f} \left(\mathbf{u}^{\mathbf{T}}\mathbf{R}\mathbf{u} + \mathbf{x}^{\mathbf{T}}\mathbf{Q}\mathbf{x}\right) dt \tag{39}$$

where $\mathbf{Q} \in \mathscr{R}^{n\times n}$, $\mathbf{R} \in \mathscr{R}^{m\times m}$ and $\mathbf{Q_f} \in \mathscr{R}^{n\times n}$ are constant matrices. Let the matrices $\mathbf{Q}$ and $\mathbf{R}$ be symmetric, nonnegative and positive definite, respectively. Let $\mathbf{Q_f}$ be a nonnegative definite matrix.

The optimal controller is given by the linear feedback law

$$\mathbf{u}(\mathbf{t})^* = -\mathbf{R}^{-1}\mathbf{G}(\mathbf{t})^{\mathbf{T}}\mathbf{P}(\mathbf{t})\mathbf{x}(\mathbf{t}) \tag{40}$$

where $\mathbf{P}(t) \in \mathscr{R}^{n\times n}$ is a symmetric matrix, satisfying the differential Riccati equation

$$-\dot{\mathbf{P}}(\mathbf{t}) = \mathbf{P}(\mathbf{t})\mathbf{F}(\mathbf{t}) + \mathbf{F}(\mathbf{t})^{\mathbf{T}}\mathbf{P}(\mathbf{t}) - \mathbf{P}(\mathbf{t})\mathbf{G}(\mathbf{t})\mathbf{R}^{-\mathbf{1}}\mathbf{G}(\mathbf{t})^{\mathbf{T}}\mathbf{P}(\mathbf{t}) + \mathbf{Q} \quad , \quad \mathbf{P}\left(t_f\right) = \mathbf{Q_f} \tag{41}$$

8 APPENDIX: ORDER REDUCTION

The guidance problem's order can be reduced by using the concept of zero effort miss (ZEM). The optimization problem is formulated as follows

$$\begin{aligned} \dot{\mathbf{x}} &= \mathbf{F}\mathbf{x} + \mathbf{G}\mathbf{u} \\ J &= \mathbf{x}^T(t_f)\mathbf{Q_f}\mathbf{x}(t_f) + \int_{t_0}^{t_f} \mathbf{u}^T\mathbf{R}\mathbf{u}\, dt \end{aligned}$$

Let $\mathbf{z}(\mathbf{t})$ denote a ZEM variable

$$\mathbf{z}(\mathbf{t}) = \mathbf{M}\Phi(\mathbf{t_f}, \mathbf{t})\mathbf{x}(\mathbf{t}) \tag{42}$$

where $\Phi(\mathbf{t_f}, \mathbf{t})$ is the transition matrix of $\mathbf{F}$, satisfying

$$\dot{\Phi}(\mathbf{t_f}, \mathbf{t}) = -\Phi(\mathbf{t_f}, \mathbf{t})\mathbf{F}, \quad \Phi(\mathbf{t_f}, \mathbf{t}) = \mathbf{I} \tag{43}$$

$\mathbf{M}$ is a constant vector, satisfying

$$\mathbf{M}^{\mathbf{T}}\mathbf{M} = \mathbf{Q_f} \tag{44}$$

Computing the time derivation of $\mathbf{z}(\mathbf{t})$

$$\dot{\mathbf{z}}(\mathbf{t}) = \mathbf{M}\dot{\Phi}(\mathbf{t_f}, \mathbf{t})\mathbf{x}(\mathbf{t}) + \mathbf{M}\Phi(\mathbf{t_f}, \mathbf{t})\dot{\mathbf{x}}(\mathbf{t}) = \mathbf{M}\Phi(\mathbf{t_f}, \mathbf{t})\mathbf{G}\mathbf{x}(\mathbf{t}) \tag{45}$$

Denote

$$\mathbf{X}(\mathbf{t_{go}}) = \mathbf{X}(\mathbf{t_f}, \mathbf{t}) = \mathbf{M}\Phi(\mathbf{t_f}, \mathbf{t})\mathbf{G}\mathbf{x}(\mathbf{t}) \tag{46}$$

Then, the reduced order optimization problem can be reformulated as follows

$$\begin{aligned} \dot{\mathbf{z}}(\mathbf{t}) &= \mathbf{X}(\mathbf{t_f}, \mathbf{t})\mathbf{u}(t) \\ J &= \|\mathbf{z}(\mathbf{t_f})\|^2 + \int_{t_0}^{t_f} \mathbf{u}^T\mathbf{R}\mathbf{u}\, dt \end{aligned} \tag{47}$$

The optimal controller takes the form

$$u^* = -\mathbf{R}^{-\mathbf{1}}\mathbf{X}^{\mathbf{T}}(\mathbf{t_{go}})\mathscr{P}\mathbf{z} \tag{48}$$

where $\mathscr{P}(\mathbf{t_{go}})$ denotes the solution to the Riccati differential equation

$$\frac{d}{dt_{go}}\mathscr{P}(\mathbf{t_{go}}) = -\mathscr{P}(\mathbf{t_{go}})\mathbf{X}\mathbf{R}^{-1}\mathbf{X}^{\mathbf{T}}\mathscr{P}(\mathbf{t_{go}}), \quad \mathscr{P}(\mathbf{0}) = \mathbf{I} \tag{49}$$

In [14] the closed form solution of a linear MIMO guidance law in the sense of $\mathscr{L}^2$ was presented.

$$\mathscr{P}(\mathbf{t_{go}}) = \left[\mathbf{I} + \int_{\mathbf{0}}^{\mathbf{t_{go}}} \mathbf{X}(\tau)\mathbf{R}^{-1}\mathbf{X}^{\mathbf{T}}(\tau)\,\mathbf{d}\tau\right]^{-1} \tag{50}$$

References

1. Shima, T., Idan, M., and Golan, O. M., "Sliding–Mode Control for Integrated Missile Autopilot Guidance," *AIAA Journal of Guidance, Control, and Dynamics*, Vol. 29, No. 2, 2006, pp. 250–260, doi:10.2514/1.14951.
2. Bryson, A. E. and Ho, Y. C., *Applied Optimal Control: Optimization, Estimation, and Control*, Hemisphere Publishing Corporation, New York, 1975, pp. 154–155.
3. Cottrell, R. G., "Optimal Intercept Guidance for Short–Range Tactical Missiles," *AIAA*, Vol. 9, No. 7, 1971, pp. 1414–1415, doi:10.2514/3.6369.
4. Shkolnikov, I., Shtessel, Y. B., and Lianos, D., "Integrated Guidance-Control System of a Homing Interceptor: Sliding Mode Approach," *Proceeding of the AIAA Guidance, Navigation, and Control Conference*, August 6–9 2001, pp. 1–11, doi:10.2514/6.2001-4218.
5. Palumbo, N. F., Reardon, B. E., and Blauwkamp, R. A., "Integrated Guidance and Control for Homing Missiles," *Johns Hopkins Apl Technical Digest*, Vol. 25, No. 2, 2004, pp. 121–139.
6. Balakrishnan, S., Stansbery, D. T., Evers, J. H., and Cloutier, J. R., "Analytical Guidance Laws and Integrated Guidance/Autopilot for Homing Missiles," *Control Applications, Second IEEE Conference*, 13-16 Sep 1993, pp. 27–32, doi:10.1109/CCA.1993.348311.
7. Park, B.-G., Kim, T.-H., and Tahk, M.-J., "Time-Delay Control for Integrated Missile Guidance and Control," *International Journal of Aeronautical and Space Science*, Vol. 12, No. 3, 2011, pp. 260–265, doi:10.5139/IJASS.2011.12.3.260.
8. Idan, M., Shima, T., and Golan, O. M., "Integrated Sliding Mode Autopilot-Guidance for Dual-Control Missiles," *AIAA Journal of Guidance, Control, and Dynamics*, Vol. 30, No. 4, 2007, pp. 1081–1089, doi:10.2514/1.24953.
9. Menon, P. K. and Ohlmeyer, E. J., "Integrated design of agile missile guidance and autopilot systems," *Control Engineering Practice*, Vol. 9, No. 10, 2001, pp. 1095–1106, doi:10.1016/S0967-0661(01)00082-X.
10. Menon, P. K., Sweriduk, G. D., and Ohlmeyer, E. J., "Optimal Fixed-Interval Integrated Guidance-Control Laws For Hit-To-Kill Missiles," *2003 AIAA Guidance, Navigation, and Control Conference*, 11-14 Aug 2003, pp. 1–9.
11. Gutman, S., Goldan, O., and Rubinsky, S., "Guaranteed Miss Distance in Guidance Systems with Bounded Controls and Bounded Noise," *AIAA Journal of Guidance, Control, and Dynamics*, Vol. 35, No. 3, 2012, pp. 816–823, doi:10.2514/1.55723.
12. Gutman, S., Shima, T., Rubinsky, S., and Levy, M., "Single vs. Two-Loop Integrated Guidance Systems," *Accepted for presentation at the CEAS Euro GNC 2013*.
13. Anderson, B. D. and Moore, J. B., *Optimal Control, Linear Quadratic Methods*, Prentice Hall, Englewood Cliffs, New Jersey, 1989, pp. 7–67.
14. Rusnak, I., Weiss, H., Eliav, R., and Shima, T., "Missile Guidance with Constained Terminal Body Angle," *2010 IEEE 26th Convention of Electrical and Electronics Engineers in Israel (IEEEI)*, 17-20 Nov 2010, pp. 45–49, doi:10.1109/EEEI.2010.5662094.